



HAL
open science

Inverse characterization of the damping performance of porous materials

Isadora R. Henriques, Lucie Rouleau, Daniel Castello, Lavinia Borges,
Jean-François Deü

► **To cite this version:**

Isadora R. Henriques, Lucie Rouleau, Daniel Castello, Lavinia Borges, Jean-François Deü. Inverse characterization of the damping performance of porous materials. *Forum Acusticum*, Dec 2020, Lyon, France. pp.3125-3129, 10.48465/fa.2020.0879 . hal-03235482

HAL Id: hal-03235482

<https://hal.science/hal-03235482v1>

Submitted on 27 May 2021

HAL is a multi-disciplinary open access archive for the deposit and dissemination of scientific research documents, whether they are published or not. The documents may come from teaching and research institutions in France or abroad, or from public or private research centers.

L'archive ouverte pluridisciplinaire **HAL**, est destinée au dépôt et à la diffusion de documents scientifiques de niveau recherche, publiés ou non, émanant des établissements d'enseignement et de recherche français ou étrangers, des laboratoires publics ou privés.

INVERSE CHARACTERIZATION OF THE DAMPING PERFORMANCE OF POROUS MATERIALS

I.R. Henriques^{1,2} L. Rouleau¹ D.A. Castello²

L.A. Borges² J.-F. Deü¹

¹ LMSSC, Conservatoire national des arts et métiers (Cnam), France

² Mech. Eng. Dept., Universidade Federal do Rio de Janeiro (UFRJ), Brazil

lucie.rouleau@lecnam.net

ABSTRACT

Porous materials are traditionally used in industry for their sound absorption and insulation properties. Over the past decade, more attention has been given to their elastic and damping properties. For instance, there is a particular interest in the automotive industry to replace heavy layers (consisting of constrained viscoelastic rubber layers) with felts or foams evidencing high damping capabilities. Hence, characterizing efficiently the viscoelastic properties of porous materials is crucial for purposes of quality control and further improvements in product development and fabrication. The goal of this work is to propose an experimental-numerical method for the inverse characterization of the frequency-dependent properties of porous materials within the Bayesian framework. To that purpose, vibration tests are first carried out on a simply supported panel with a free-layer of closed-cell polyurethane foam in the low-frequency range. Then, a finite element model is developed considering only the viscoelasticity of the porous skeleton, neglecting the influence of the fluid phase. A four-parameter fractional derivative model is calibrated and validated using a probabilistic approach. Furthermore, the results of this inverse characterization are compared to the viscoelastic properties identified by dynamical mechanical analysis.

1. INTRODUCTION

Porous materials have recently gained attention due to their potential capacity to be used for purposes of vibration control, without significantly influencing the weight of the structure [1–4]. Hence, the determination of their mechanical properties has become crucial in the prediction of their damping performance.

Direct measurement of all properties often requires different testing equipment, and this could be troublesome in some sense. Therefore, inverse methods have been increasingly used in the characterization of materials. Among the different approaches available in the literature, a probabilistic identification seems more reasonable as it can deal with uncertainties of experimental measurements and numerical models which are based on assumptions and approximations [5,6].

Bearing this in mind, this work proposes an

experimental-numerical procedure for the inverse characterization within the Bayesian framework of the viscoelastic properties of porous materials, in particular a closed-cell polyurethane foam. For this reason, vibrational tests are first carried out on a two-layered simply supported panel, as shown in Fig. 1, in the low-frequency range. A finite element model is then implemented considering only the viscoelasticity of the porous skeleton. A four-parameter fractional derivative model is calibrated within Bayesian framework. The results of this inverse characterization are compared with the ones identified by a dynamic mechanical analysis [4].

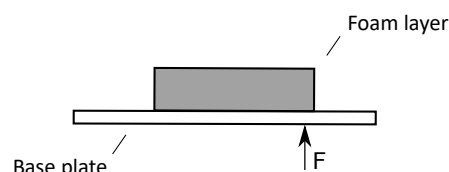


Figure 1: Configuration of simply supported panel.

This work is organized as follows. Section 2 introduces the constitutive model and the finite element formulation. Then, Section 3 presents the inverse formulation adopted to estimate the viscoelastic properties. Afterward, Section 4 describes the experimental set-up. Finally, Section 5 presents the results, followed by concluding remarks.

2. NUMERICAL MODEL

2.1 Finite element formulation

Under the paradigm of modeling porous materials, the dissipation of mechanical energy due to the viscoelasticity of the solid skeleton is often the main source of damping in the low-frequency range [2, 4, 7]. Therefore, the porous material is herein assumed to be as a homogeneous viscoelastic one.

The finite element discretisation of the differential equations of a general problem consisting in a vibrating elastic structure bonded to a viscoelastic layer results in the following equation of motion

$$[\mathbb{K}_E + G^*(\omega)\mathbb{K}_V^0 - \omega^2\mathbb{M}]U(\omega) = F(\omega), \quad (1)$$

where \mathbb{K}_E is the global stiffness matrix related to elastic component, \mathbb{K}_V^0 is the global stiffness matrix associated with the viscoelastic layer and evaluated for a unitary shear modulus, $G^*(\omega)$ is the complex shear modulus of the viscoelastic material, \mathbb{M} is the global mass matrix, $\mathbf{U}(\omega)$ and $\mathbf{F}(\omega)$ are, respectively, the displacement and force vectors in the frequency domain.

As for the complex shear modulus $G^*(\omega)$, it is assumed herein a four-parameter fractional derivative model (FPFDM), also known as fractional Zener model, due to its capability of providing good predictions of the behavior of the investigated foam [4, 7]. It is thus expressed as follows [8, 9]

$$G^*(\omega) = \frac{G_0 + G_\infty(j\omega\tau)^\alpha}{1 + (j\omega\tau)^\alpha} \quad (2)$$

where G_0 and G_∞ are, respectively, the relaxed and unrelaxed shear moduli, τ is the relaxation time and α is the order of the fractional derivative model. It is worthwhile mentioning that these four parameters must follow thermodynamical constraints such as $G_\infty > G_0 > 0$, $\tau > 0$, and $0 < \alpha \leq 1$, and must be estimated by inverse techniques.

It is worth noting that the hypotheses of isotropy and constant Poisson's ratio ν are also adopted for the investigated foam. In this way, all foam's mechanical moduli are independent of the direction and also have the same frequency dependence. As a consequence, a three-dimensional constitutive law can be implemented as follows

$$\mathbb{C}^*(\omega) = G^*(\omega) \begin{bmatrix} \frac{2(1-\nu)}{1-2\nu} & \frac{2\nu}{1-2\nu} & \frac{2\nu}{1-2\nu} & 0 & 0 & 0 \\ \frac{2\nu}{1-2\nu} & \frac{2(1-\nu)}{1-2\nu} & \frac{2\nu}{1-2\nu} & 0 & 0 & 0 \\ \frac{2\nu}{1-2\nu} & \frac{2\nu}{1-2\nu} & \frac{2(1-\nu)}{1-2\nu} & 0 & 0 & 0 \\ \frac{2\nu}{1-2\nu} & \frac{2\nu}{1-2\nu} & \frac{2\nu}{1-2\nu} & 0 & 0 & 0 \\ 0 & 0 & 0 & 1 & 0 & 0 \\ 0 & 0 & 0 & 0 & 1 & 0 \\ 0 & 0 & 0 & 0 & 0 & 1 \end{bmatrix}, \quad (3)$$

where $\mathbb{C}^*(\omega)$ is the constitutive matrix of the material.

2.2 Numerical implementation

An in-house program combining GMSH [10] and MATLAB[®] software is used to build the geometries together with the corresponding meshes, and also to compute the frequency response functions (FRFs) using the multi-model approach [11].

The investigated structure is modeled with the 20-node hexahedral elements since they can describe better some physical mechanisms of viscoelastic layers. This resulted in 14241 degrees of freedom.

3. BAYESIAN INVERSION METHOD

The goal of the inverse method is to estimate the parameters of the fractional derivative model chosen to describe

the viscoelastic behavior of the porous material, namely $\{G_0, G_\infty, \tau, \alpha\}$. For this, a probabilistic approach based on the Bayesian inference is considered to assess information about the parameters.

The central idea behind this approach is to obtain all possible information about the unknown parameters θ consistently with (i) the set of measured data \mathbf{Y} , (ii) the mathematical model, and (iii) the information about θ before the measurements. The problem solution corresponds to the posterior probability density function (PDF) for θ given the available data \mathbf{Y} .

In this regard, all unknown quantities and measurements are considered as random variables. The uncertainty about each random variable is modeled through its PDF.

From a mathematical standpoint, parameter estimation within the Bayesian framework relies on the Bayes' theorem [5, 6]

$$\pi(\theta|\mathbf{Y}) \propto \pi(\mathbf{Y}|\theta)\pi_0(\theta) \quad (4)$$

where $\pi(\theta|\mathbf{Y})$ is the posterior probability density function of the model parameters, $\pi(\mathbf{Y}|\theta)$ is the likelihood function and $\pi_0(\theta)$ is the prior model adopted for the unknown parameters θ .

Once the posterior PDF $\pi(\theta|\mathbf{Y})$ is built, one can compute point estimates for θ such as the maximum a posteriori (MAP) estimator θ_{MAP} and also explore this through sampling based techniques such as Markov Chain Monte Carlo (MCMC) method.

3.1 Choice of the likelihood function

The likelihood function $\pi(\mathbf{Y}|\theta)$ is related to the uncertainty of measuring \mathbf{Y} . Its specification depends on the hypotheses about the distribution of noise [5, 6]. In this work, it is assumed that this uncertainty takes the form of an additive noise described by a Gaussian distribution with zero mean and unknown variance σ^2 such as $\epsilon \sim N(0, \sigma^2)$. Therefore, it may be represented as

$$\pi(\mathbf{Y}|\theta) = \frac{1}{(2\pi\sigma^2)^{N_y/2}} \exp\left\{-\frac{[\mathbf{Y} - f(\theta, \mathbf{x})]^2}{\sigma^2}\right\}. \quad (5)$$

3.2 Choice of the prior probability distribution

The prior PDF $\pi_0(\theta)$ is used to describe the users' beliefs about model parameters prior to measurements [5, 6]. In this work, it is assumed that the parameters are mutually independent, i.e., $\pi_0(\theta) = \pi_0(\theta_1) \times \dots \times \pi_0(\theta_N)$. Each PDF $\pi_0(\theta_i)$ is modeled as a uniform distribution such that $\pi_0(\theta_i) \sim U(a_i, b_i)$. Moreover, the constraints of the problem are imposed through the supports a_i and b_i .

3.3 Markov chain Monte Carlo method

Markov Chain Monte Carlo (MCMC) method is any computational approach used to explore the posterior PDF based on the ideas of Monte Carlo integration and Markov chains. Generally speaking, it consists in generating samples from an ergodic Markov chain $\{\theta^{(1)}, \theta^{(2)}, \dots, \theta^{(M)}\}$

whose stationary distribution corresponds to the posterior PDF $\pi(\theta|\mathbf{y})$. These samples are generated sequentially such that the sample distribution $\theta^{(j)}$ depends only on the last generated sample $\theta^{(j-1)}$ [5, 6].

Several algorithms can be found in literature [5, 6]. It is considered herein the Delayed Rejection Adaptive Metropolis (DRAM) algorithm [12] aiming at improving the efficiency of the method. This particular algorithm combines the main characteristics of the Adaptive Metropolis (AM) and Delayed Rejection (DR) algorithms, retaining the Markovian property and reversibility of the Markov chains.

4. EXPERIMENTAL SET-UP

The system under analysis is a two-layered panel mounted in frame to approximate simply supported conditions [13] as shown in Fig. 2. The geometric and physical characteristics of the base plate and the porous material are detailed next on Tab. 1. The free-layer of porous materials corresponds to a closed-cell polyurethane foam previously characterized by Bonfiglio *et al.* [14] and by Henriques *et al.* [4].

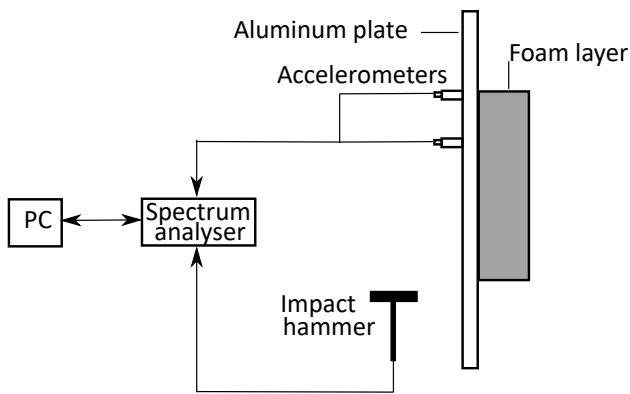
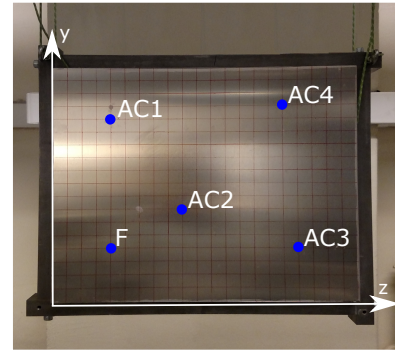


Figure 2: Experimental set-up.

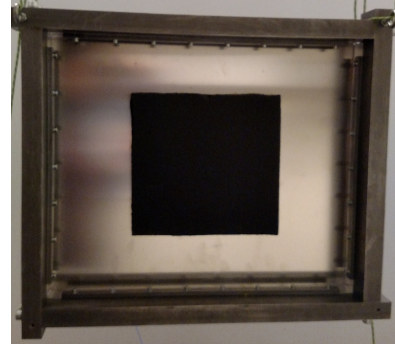
Table 1: Description of the components of the simply supported panel.

Description	Aluminum	Polyurethane foam
ρ [kg/m ³]	2700	48
ν	0.3	0.35
E [GPa]	69	-
Thickness [mm]	3	25
Width [mm]	360	200
Length [mm]	420	200

An impact hammer is used to apply a point force (F) at coordinates (0 mm, 80 mm, 80 mm) to excite the panel and four accelerometers ($AC1, AC2, AC3, AC4$) are glued on the bare panel side through beeswax in different locations to measure the structure's response, as illustrated in Fig. 3. Measurements are thus performed up to 800 Hz, with a frequency step of 0.5 Hz, at room temperature.



(a) Location of the applied force and accelerometers



(b) Foam layer glued on aluminum plate

Figure 3: Photographs of simply supported panel.

It should be pointed out that vibration tests on the bare aluminum panel have been conducted to perform a model updating process to take into account, for example, imperfections in the realization of the boundary conditions.

5. RESULTS

As previously mentioned, the unknown parameters were defined as $\theta = \{G_0, G_\infty, \tau, \alpha\}^T$. These parameters, however, vary some orders of magnitude for the investigated material according to the results presented by Bonfiglio *et al.* [14] and by Henriques *et al.* [4]. For this reason, they were normalized $\theta = \{p_1, p_2, p_3, p_4\}^T$ to enhance the performance of this estimation [6] such as

$$p_1 = G_0 \times 10^{-4} [\text{Pa}], \quad (6a)$$

$$p_2 = G_\infty \times 10^{-6} [\text{Pa}], \quad (6b)$$

$$p_3 = \tau \times 10^{-8} [\text{s}], \quad (6c)$$

$$p_4 = \alpha. \quad (6d)$$

The experimental data comprised the FRFs measured by the four accelerometers $\{AC1, AC2, AC3, AC4\}$. Since the model updating process must be independent of model validation, a specific organization was thus adopted. Firstly, the measured data has been split into two groups such that the calibration was performed using the FRFs measured by accelerometers $\{AC1, AC2\}$, and the model validation was quantified using the FRFs measured by accelerometers $\{AC3, AC4\}$. Then, the

complex FRF measured by an accelerometer AC_i was organized in a N -dimensional vector such as $\tilde{\mathbf{H}}|_{AC_i} = \{\tilde{H}(\omega_1)|_{AC_i}, \dots, \tilde{H}(\omega_N)|_{AC_i}\}^T$. Finally, the measured data \mathbf{Y} used during model updating corresponded to a $4N$ -dimensional vector defined as follows

$$\mathbf{Y} = \{\Re[\tilde{\mathbf{H}}|_{AC_1}]^T \Re[\tilde{\mathbf{H}}|_{AC_2}]^T \Im[\tilde{\mathbf{H}}|_{AC_1}]^T \Im[\tilde{\mathbf{H}}|_{AC_2}]^T\}^T \quad (7)$$

where $\Re[\tilde{\mathbf{a}}]$ and $\Im[\tilde{\mathbf{a}}]$ are, respectively, the real and imaginary parts of a complex vector $\tilde{\mathbf{a}}$.

It is important to highlight that the calibration step did not consider all the experimental points obtained in the measurements. Only the experimental points related to the resonance peaks and ten more points linearly-spaced frequency grids located around each resonance peak were selected. This strategy allowed us to improve the computational time of the problem.

The posterior PDF of the unknown parameters was thus explored using the DRAM algorithm, which generated a total of 50000 samples. The convergence of the algorithm to the stationary posterior PDF was assessed by computing the cumulative mean in the Markov chain of all the parameters, and also by observing the well-mixing behavior of the chains.

Table 2 shows the posterior mean value $\mathbb{E}[\theta]$ together with the 95 % credibility interval (CI) of the unknown parameters θ obtained with this MCMC method.

Table 2: Posterior mean value and 95 % credibility interval (CI) of the unknown parameters θ .

Material Parameter	$\mathbb{E}[\theta]$	95 % CI
G_0 [$\times 10^4$ Pa]	1.09	[0.59, 1.89]
G_∞ [$\times 10^6$ Pa]	2.66	[1.45, 4.42]
τ [$\times 10^{-8}$ s]	4.42	[3.09, 5.88]
α	0.42	[0.35, 0.49]

Figure 4 shows the uncertainty propagation from the model parameters $\theta \sim \pi(\theta|\mathbf{Y})$ to the structure's frequency response function $\tilde{\mathbf{H}}$. It can be seen a good agreement, on the whole, between the calibrated model and the experimental data. The credibility intervals were quite narrow for most of the frequency range. Higher uncertainties appeared after approximately 680 Hz and this difficulty may be related to the multi-model approach used to compute the FRFs in the uncertainty propagation.

To validate the estimated parameters, the uncertainty propagation was performed for the FRFs of the two accelerometers AC_3 and AC_4 , which were not used in calibration. Figure 5 compares the 95 % credibility interval for the calibrated FPFDM and the measured data from accelerometer AC_3 . A good agreement can be observed in this prediction.

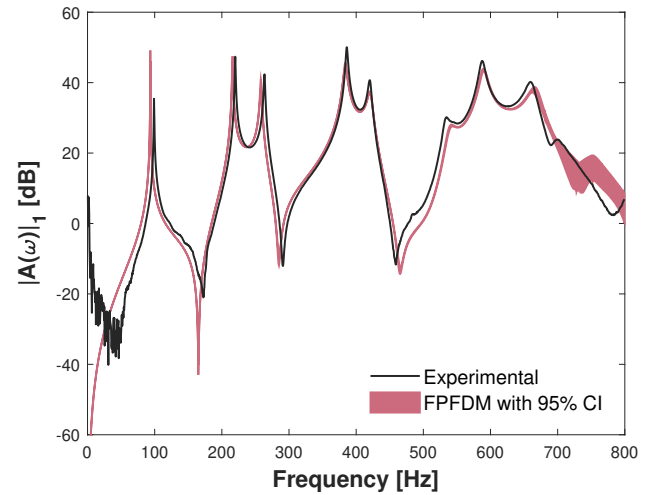


Figure 4: Uncertainty propagation when considering $\theta \sim \pi(\theta|\mathbf{Y})$ for the FRF of accelerometer AC_1 .

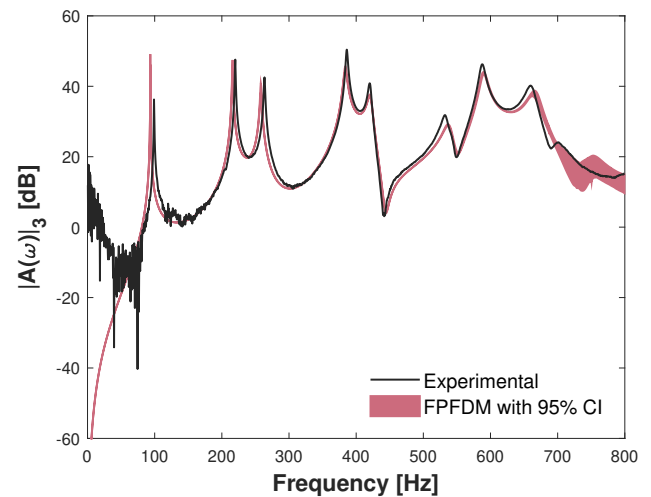


Figure 5: Uncertainty propagation when considering $\theta \sim \pi(\theta|\mathbf{Y})$ for the FRF of accelerometer AC_3 .

To further evaluate the efficiency of the proposed inverse identification, the results obtained are compared with the ones estimated by Henriques *et al.* [4] using measured data from DMA as shown in Tab. 3. It is possible to observe that the average values estimated for the parameters G_∞ and α are more discrepant (in percentage terms) when compared to those estimated by the DMA. Nevertheless, if one considers the credibility intervals shown in Tab. 2, all estimated parameters had a good agreement with each other.

Table 3: Comparison between the MCMC results and the ones estimated using measured data from DMA [4].

Material Parameter	MCMC	DMA
G_0 [$\times 10^4$ Pa]	1.09	1.31
G_∞ [$\times 10^6$ Pa]	2.66	2.11
τ [$\times 10^{-8}$ s]	4.42	4.70
α	0.42	0.30

6. CONCLUSION

In this work, an inverse characterization procedure was proposed to estimate the viscoelastic properties of porous material based on the Bayesian framework. The inherent uncertainties from model assumptions and experimental measurements could be quantified. The estimated parameters were expressed by a probability density function, allowing the determination of some statistics such as the mean. Stochastic models could be computed, showing good levels of correlation with measured data.

7. REFERENCES

- [1] M. A. Rodríguez-Pérez and J. A. De Saja, “Dynamic mechanical analysis applied to the characterisation of closed cell polyolefin foams,” *Polymer Testing*, vol. 19, pp. 831–848, 2000.
- [2] N. Dauchez, S. Sahraoui, and N. Atalla, “Investigation and modelling of damping in a plate with a bonded porous layer,” *Journal of Sound and Vibration*, vol. 265, no. 2, pp. 437–449, 2003.
- [3] T. Ehrig, N. Modler, and P. Kostka, “Compression and frequency dependence of the viscoelastic shear properties of flexible open-cell foams,” *Polymer Testing*, vol. 70, no. June, pp. 151–161, 2018.
- [4] I. R. Henriques, L. Rouleau, D. A. Castello, L. A. Borges, and J. F. Deü, “Viscoelastic behavior of polymeric foams: Experiments and modeling,” *Mechanics of Materials*, vol. 148, 2020.
- [5] J. P. Kaipio and E. Somersalo, *Statistical and computational inverse problems*, vol. 160. 2005.
- [6] R. C. Smith, *Uncertainty quantification: theory, implementation, and applications*. Philadelphia: Society for Industrial and Applied Mathematics, 2013.
- [7] I. Henriques, L. Rouleau, D. Castello, L. Borges, and J. F. Deü, “Damping performance of porous materials through dynamic analysis,” in *48th International Congress and Exhibition on Noise Control Engineering*, (Madrid), 2019.
- [8] R. L. Bagley and P. J. Torvik, “A Theoretical Basis for the Application of Fractional Calculus to Viscoelasticity,” *Journal of Rheology*, vol. 27, no. 3, pp. 201–210, 1983.
- [9] R. L. Bagley and P. J. Torvik, “On the Fractional Calculus Model of Viscoelastic Behavior,” *Journal of Rheology*, vol. 30, no. 1, pp. 133–155, 1986.
- [10] C. Geuzaine and J. Remacle, “Gmsh: A 3-D finite element mesh generator with built-in pre- and post-processing facilities,” *Int. J. Numer. Methods Eng.*, vol. 79, no. 11, pp. 1309–1331, 2009.
- [11] L. Rouleau, J. F. Deü, and A. Legay, “A comparison of model reduction techniques based on modal projection for structures with frequency-dependent damping,” *Mechanical Systems and Signal Processing*, vol. 90, pp. 110–125, 2017.
- [12] H. Haario, M. Laine, A. Mira, and E. Saksman, “DRAM: Efficient adaptive MCMC,” *Statistics and Computing*, vol. 16, no. 4, pp. 339–354, 2006.
- [13] O. Robin, J.-D. Chazot, R. Boulandet, M. Michau, A. Berry, and N. Atalla, “A Plane and Thin Panel with Representative Simply Supported Boundary Conditions for Laboratory Vibroacoustic Tests,” *Acta Acustica united with Acustica*, vol. 102, pp. 170–182, 2016.
- [14] P. Bonfiglio, F. Pompoli, K. V. Horoshenkov, M. I. B. A. Rahim, L. Jaouen, J. Rodenas, F. X. Bécot, E. Gourdon, D. Jaeger, V. Kursch, M. Tarello, N. B. Roozen, C. Glorieux, F. Ferrian, P. Leroy, F. B. Vangosa, N. Dauchez, F. Foucart, L. Lei, K. Carillo, O. Doutres, F. Sgard, R. Panneton, K. Verdiere, C. Bertolini, R. Bär, J. P. Groby, A. Geslain, N. Poulain, L. Rouleau, A. Guinault, H. Ahmadi, and C. Forge, “How reproducible are methods to measure the dynamic viscoelastic properties of poroelastic media?,” *Journal of Sound and Vibration*, vol. 428, pp. 26–43, 2018.